VHF HIGH REPETITION RATE PHOTOINJECTOR DESIGN FOR THE NLS PROJECT

J.W. McKenzie* & B.L. Militsyn, STFC Daresbury Laboratory, Warrington, WA4 4AD, UK

Abstract

Future FEL-based light sources require high brightness electron beams delivered in short bunches at high repetition rates. The design of a photoinjector able to operate at a repetition rate of 1 MHz and above is presented. Beam dynamic simulations are presented for bunch charges ranging from 100 pC up to 1 nC, optimised for low slice emittance and high peak current. This injector is a suitable candidate for the UK's New Light Source project.

INTRODUCTION

Low emittance electron beams delivered at a high repetition rate are desired for several future FEL-based light source projects including the UK's New Light Source (NLS) [1]. Currently operational linac-based FELs such as LCLS [2] and FLASH [3] use 1.5 cell pulsed normal conducting RF guns operating at the frequency of the main linac. These have delivered beams with emittance values down to 0.3 mm mrad [2], however are limited in repetition rate due to cavity heating. The first stage of NLS will use an L-band RF photoinjector utilising a modified PITZ gun [1], however this is unable to deliver repetition rates up to 1 MHz as desired by the science case for the project.

As reported in [1,4], three options present themselves for a high repetition rate gun. High voltage DC guns, which have been used for ERL-based IR-FELs such as that at Jefferson Laboratory [5], are able to operate up to the linac frequency. However, their emittance is limited because the maximum achievable field strength available on the photocathode is less than 5 MV/m, due to parasitic field emission. Superconducting RF guns, such as [6], should be able to operate in CW mode and provide similar performance to existing normal conducting RF guns however this has yet to be demonstrated experimentally.

A further alternative is a relatively low frequency, large cavity, normal conducting RF gun such as that proposed by LBNL [7]. This operates at a fundamental frequency of 187 MHz and the low power density allows this to potentially run in CW mode. The cavity features a re-entrant geometry, thus has a small anode-cathode gap, leading to beam dynamics similar to DC guns. A field gradient of 20 MV/m should be achievable on the photocathode, providing a lower emittance than DC guns.

The result of beam dynamic simulations of a VHF gun based injector is presented here at a range of bunch charges, with the focus being on 200 pC, as required for NLS, and a discussion on the various photocathodes that can be considered.

INJECTOR LAYOUT

Since the 750 keV beam produced from the VHF gun is similar to a high voltage DC gun, a similar injector layout is proposed. A focussing solenoid is located just after the gun cavity, with a bucking solenoid built as part of the gun construction. A 1.3 GHz single cell normal-conducting buncher cavity is followed by a second solenoid. A superconducting booster based on two 1.3 GHz 9-cell Tesla cavities may be realized by the first cavities of the main linac or built in a separate cryomodule.
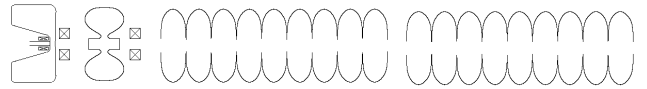

Figure 1: Schematic injector layout.

SIMULATIONS

Laser pulse optimisation

In order to reduce the complexity of the optimisation of the injector beamline, the profile of the drive laser pulse was optimised separately. ASTRA simulations were carried out using a multi-objective genetic algorithm utilising the non-dominating sorting technique. The laser profile was set with both top-hat transverse and temporal distributions, with the full length of the laser pulse allowed to vary from 10 to 120 ps and the spot diameter from 0.4 to 10 mm. The field of the initial focussing solenoid was also included, ranging from 0 – 0.1 T with the bucking coil set accordingly to zero the magnetic field on the cathode plane.
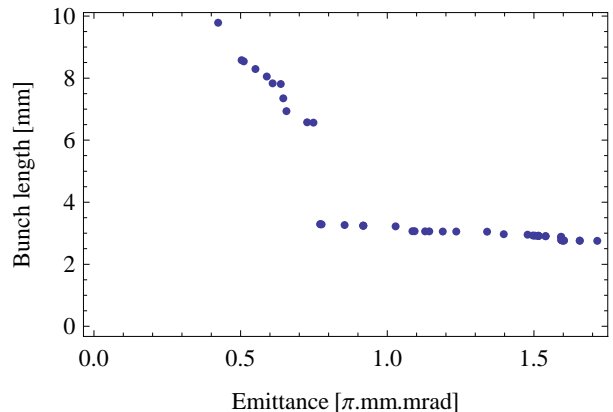

Figure 2: Projected transverse rms emittance against rms bunch length for varying the laser pulse for a 200 pC beam.

The optimisation parameters were the projected transverse emittance and bunch length. Figure 2 shows the Pareto-like front after 24 generations with a population size of 60 for a bunch charge of 200 pC. As seen, the minimum emittance achievable is just over 0.4 mm mrad but with a longer bunch length. The solutions are arranged in two regimes. Those which use a long (60 – 100 ps) laser pulse and achieve lower emittance but with long bunch length and those which opt for the shortest laser pulse length (and smallest diameter) as the simulation limits were set to and simply vary the solenoid setting to change the emittance compensation.

The solutions with the lowest emittances, below 0.5 mm mrad, utilise a laser pulse with large diameter, above 6 mm. However, these simulations did not include thermal emittance, and since thermal emittance scales linearly with laser spot diameter (see Equation 1), small diameters are preferable. The solution with the lowest emittance and smallest laser spot size is that with a laser pulse length of 90 ps and spot diameter of 2 mm which produces a beam with emittance 0.59 mm mrad with an rms bunch length of 8 mm. This laser pulse was chosen for the simulations of the complete injector.

Injector optimisation

To optimise the setup of the injector beamline, the same evolutionary algorithm was used, again optimising projected transverse emittance against bunch length, varying the field strengths, phases, and distances between beamline components. Simulations were carried out using only 1000 macroparticles to cut down computing time thus eliminating the possibility to set the optimiser for slice emittance and peak current directly as the slice-to-slice noise is too high to get meaningful results. Instead, once a satisfactory Pareto-like front is found, the optimiser was stopped and the top rank solutions were re-ran with 10,000 macroparticles in order to produce a slice analysis. Then the solutions were checked for smooth longitudinal phase space, short bunches, and low slice emittance over a large portion of the bunch.

Table 1: Beam parameters for: A – post booster, no thermal energy, B – post booster, 0.7 eV thermal energy, C – post first linac module, 0.7 eV thermal energy

Parameter	Units	A	B	C
Projected emittance	mm mrad	1.06	1.17	1.15
Average slice emit.	mm mrad	0.55	0.75	0.75
Peak current slice emit.	mm mrad	0.45	0.65	0.67
Bunch length (rms)	ps	6.7	6.7	6.7
Energy	MeV	10	10	115

Figure 3 shows the parameters of the final selected bunch and Table 1 shows the beam parameters at the exit of the booster for the chosen solution. As can be seen, although the projected transverse emittance is relatively large (just over 1 mm mrad) the average slice emittance is 0.55 mm mrad, with the bulk of the beam at a low emittance bar a large spike at the tail and a smaller spike at the head. The emittance corresponding to the slice of

peak current is 0.45 mm mrad. The longitudinal phase space features the required chirp for a downstream magnetic chicane compression system however features curvature which requires the use of a third harmonic cavity to linearise.
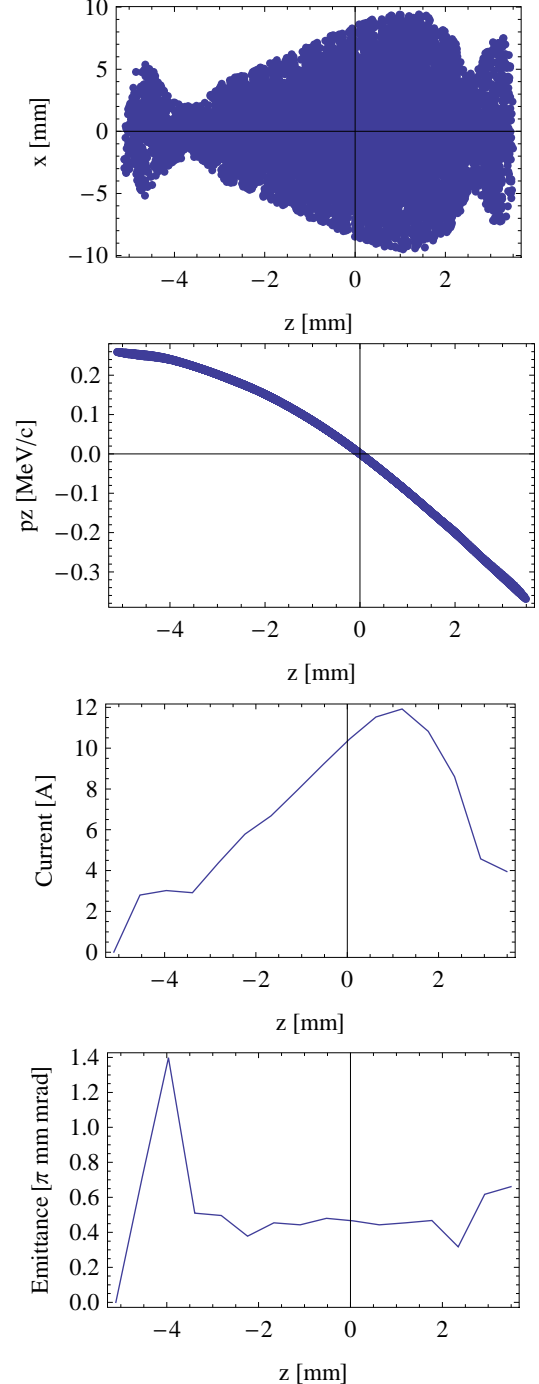

Figure 3: Beam distribution, longitudinal phase space, current profile and slice emittance for a beam after the booster cavity with zero thermal emittance.

Buncher cavity

A simulation has also been carried out using a subharmonic 650 MHz buncher cavity in place of the 1.3 GHz cavity. Set to half the peak field of the 1.3 GHz

cavity, the subharmonic buncher delivered identical performance for the laser pulse length of 90 ps with no change in longitudinal phase space. Therefore we see no reason to use a subharmonic bunching cavity as that only complicates the RF infrastructure. It should also be noted that the simulated 1.3 GHz buncher cavity requires a peak field of 4.5 MV/m in a single cell cavity. This may not be feasible and a multi-cell cavity may be needed.

Post-linac phase space

A further ASTRA simulation has been carried out to include the first linac module of NLS to ensure that the beam properties did not alter upon further acceleration. The phases of the eight 9-cell Tesla cavities were set to -20°. The results are shown in Table 1, and Figure 4 shows a reduction in curvature of the longitudinal phase space of the beam compared to after the booster.
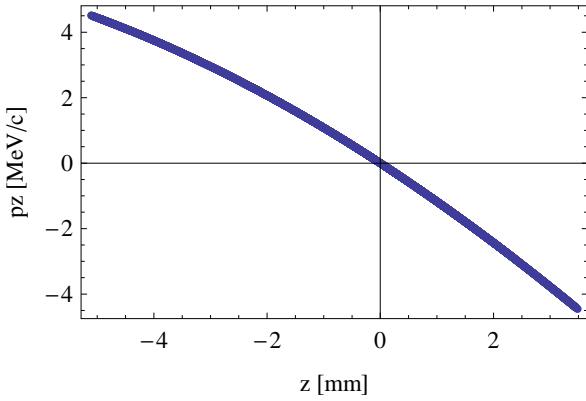

Figure 4: Longitudinal phase space of the 115 MeV bunch after the first linac module.

Thermal emittance

The optimisation was done without including initial thermal emittance. Thermal emittance, ε_{th}, can be included in ASTRA as

$$\varepsilon_{th} = \frac{r}{2}\sqrt{\frac{3}{2}\frac{k_B T}{m_0 c^2}} \qquad (1)$$

given the assumption of isotropic emission of electrons of energy $k_B T$ from the photocathode into a hemisphere of radius r [8].

Including thermal emittance in the ASTRA simulations shows no significant effect on any of the beam parameters and distributions apart from the emittance. Figure 5 shows how the emittance of the optimised injector at the exit of the booster module increases with initial thermal energy in a range of $0 - 2$ eV.

It was found that better results were obtained by adding thermal emittance post-optimisation rather than optimising including thermal emittance. This could largely be explained due to the large difference between slice and projected emittance. This also leaves the optimisation independent of photocathode choice.

Figure 6 shows the slice emittance when the beam has initial thermal energy of 0.7 eV – the value used in NLS calculations for Cs$_2$Te photocathodes [1].
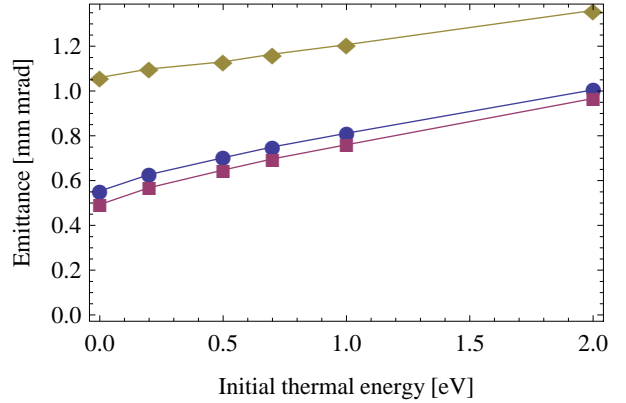

Figure 5: Emittance at the exit of the booster module against initial thermal energy. The top line is projected emittance, the middle line average slice emittance, and the bottom line emittance of the slice of peak current.
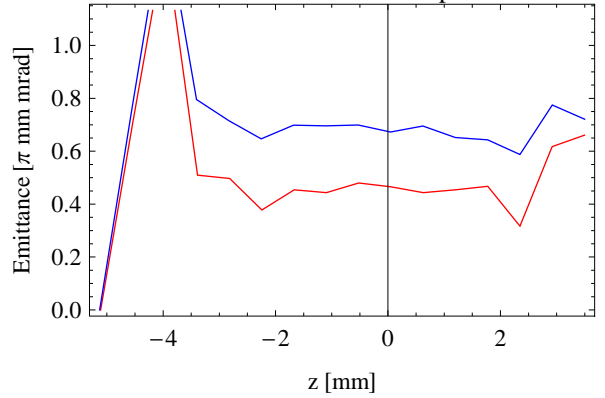

Figure 6: Slice emittance comparison between no thermal emittance (red) and that corresponding to an initial energy of 0.7 eV (blue) for Cs$_2$Te photocathodes.

Injector performance at various bunch charges

To investigate the performance of the injector at different bunch charges the optimisation procedure was performed as above but with the location of the beamline elements fixed from the 200 pC case. The laser pulse length was kept at 90 ps for all charges except 1 nC where it was extended to 100 ps. The laser spot diameter was increased from 2 mm for the 100 pC and 200 pC cases up to 4 mm for 500 pC and 5 mm for 1 nC.
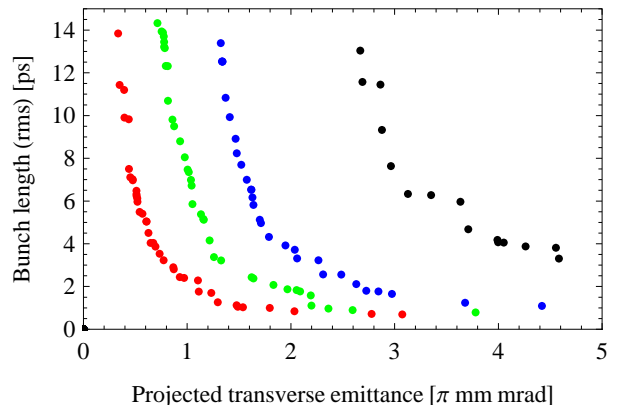

Figure 7: Optimisation curves for 100 pC (red), 200 pC (green), 500 pC (blue) and 1 nC (black).

Figure 7 shows the Pareto-like fronts for the various charges with zero thermal emittance after running the optimiser for roughly 60 generations with a population size of 60 for each case. It can clearly be seen that the performance of the injector is highly dependent on bunch charge. Therefore this kind of injector is ideally suited to high average current, low charge machines such as ERLs and less suitable for high charge, low emittance operation.

PHOTOCATHODE CHOICES

Currently two groups of photocathodes are used in FEL injectors – metallic and semiconductor. Metallic photocathodes are very fast, very robust and do not require extra-high vacuum conditions. They last for a long time but have low quantum efficiency (QE) of 10^{-5} - 10^{-3}. They operate with ultra-violet (UV) light, typically 266 nm, where the maximum average laser power yet achieved does not exceed 1 W. The maximum average current achievable with metallic photocathodes lays in the µA-region, which rules out their use for NLS.

Among the numerous known semiconductor photocathodes, two groups are widely used in accelerator applications – III-V photocathodes, the most widespread being GaAs, and alkali photocathodes such as Cs_2Te.

GaAs family photocathodes are typically used in DC guns for production of polarised electrons and are candidates for high current (100 mA) ERL injectors. The typical QE of GaAs at a wavelength of 532 nm is 1 – 10 % and they are potentially able to deliver 100 mA of high brightness beam. At Cornell University an average current of 22 mA has been obtained [9]. GaAs has extremely high demands on operational vacuum conditions – pressure in a typical GaAs gun is at the level of 10^{-11} mbar. Several attempts to implement GaAs in RF guns have yet not led to success. Low lifetime is also an issue. The dominant mode of GaAs degradation is bombardment of its surface by a back stream of ions, and the typical lifetime expressed in terms of total extracted charge is less than 500 C. Preparation of GaAs is a very complicated and expensive procedure and can not be justified by the poor performance of the photocathodes in the injectors similar to the one required for NLS.

The second group of semiconductor photocathodes considered here are alkali photocathodes. Cs_2Te is a very popular photocathode and has demonstrated relatively high QE of 1 – 10 % at a wavelength of 266 nm. The high robustness of the Cs_2Te allows it for being used in pulsed RF guns. It is also used in the DC-SRF gun at Peking University [10]. The material has demonstrated good performance at FLASH [3] and at PITZ [11] delivers 1 nC bunches in 700 µs trains with a repetition rate of 1 MHz. Potentially Cs_2Te is able to deliver the required NLS average current, but the power of the UV laser required for reliable operation is on the brink of state of the art and does not provide good contingency. Effects of photocathode degradation and the maximum charge which may be extracted from the sample are also not completely investigated.

The second group of alkali photocathodes are antimonite based photocathodes including Cs_3Sb, K_2CsSb and NaKCsSb (S-20). They have been used for years in photo-multiplier tubes and vacuum photodiodes and have demonstrated a QE of 15 – 20 % at a wavelength of 532 nm. K_2CsSb was used in the "Boeing gun" which has demonstrated the highest average current extracted from a photocathode of 32 mA [12]. Unfortunately, antimonite based photocathodes are not widely used in photoinjectors because of their complicated preparation procedure and relatively low robustness (better than GaAs but worse than Cs_2Te). The mode of their degradation and the maximum extracted charge are also not very well understood.

CONCLUSION

A VHF gun with an alkali photocathode is a suitable candidate for a 1 MHz NLS injector. Simulations show a slice emittance of 0.65 mm mrad that meets the requirement for NLS, although it is higher than the 0.3 mm mrad of the stage one L-band injector [1] due to lower field strength on the photocathode.

ACKNOWLEDGEMENTS

REFERENCES

[1] "*NLS Project: Science Case & Outline Facility Design*", available at http://www.newlightsource.org

[2] P. Emma, "*First lasing of the LCLS X-Ray FEL at 1.5 Å*", proceedings of PAC 2009.

[3] K. Honkavaara et al., "*Status of FLASH*", proceedings of FEL 2008.

[4] B.L. Militsyn et al., "High repetition rate electron injectors for FEL-based next generation light sources", proceedings of LINAC 2008.

[5] D. Douglas, "The Jefferson Lab 1 kW IR FEL", proceedings of LINAC 2000.

[6] J. Teichert et al., "*Initial commissioning experience with the superconducting RF photoinjector at ELBE*", proceedings of FEL 2008.

[7] F. Sannibale et al., "Status and plans for the LBNL normal-conducting CW VHF photo-injector", these proceedings.

[8] K. Flöttmann, "Note on the thermal emittance of electrons emitted by cesium telluride photo cathodes", TESLA-FEL report 1997-01.

[9] Bruce Dunham, private communication.

[10] R. Xiang et al., "*Experimental investigations of DC-SC photoinjector at Peking University*", NIM A 527 (2004) 321-325.

[11] F. Stephan et al., "*New experimental results from PITZ*", proceedings of LINAC 2008

[12] D.H. Dowell et al., "*Results from the average power laser experiment photocathode injector test*", NIM A 356 (1995) 167-176.